Evaporation Rates of Volatile Liquids in a Laminar Flow System

Part I. Pure Liquids

MICHAEL W. CLARK and C. JUDSON KING

University of California, Berkeley, California

Normal pentane and isopentane were evaporated into nitrogen in laminar, concurrent flow in a rectangular channel. Composition profiles within the gas phase were measured, and the evaporation rates were compared with theoretical predictions with satisfactory agreement. The interfacial mole fraction of the evaporating species in the gas phase ranged as high as 0.74. A solution is reported for the Leveque problem under high flux conditions.

The rate of evaporation of a pure liquid into an adjacent laminar flowing gas stream can usually be predicted by solving a simplified form of the equation of convective diffusion written for the gaseous phase. If the vapor pressure of the liquid is sufficiently high, correction factors must be applied to the mass transfer coefficients which one would use for the situation of low concentration level and low mass flux. A second problem which is encountered as the liquid volatility increases stems from the interaction of heat and mass transfer. As the mass transfer rate increases, the enthalpy change of evaporation brings about a reduction in both the interfacial temperature and, consequently, the liquid vapor pressure at the interface. The result is a reduction in the mass transfer rate compared with that which would be predicted by ignoring this effect.

The purpose of this study has been to investigate the evaporation of a volatile liquid in an experimental system for which the fluid dynamics of both phases, as well as the low flux and low concentration-level transfer coefficients, are well known. Part II of this work deals with these phenomena, in regard to evaporation from liquid mixtures, where the resistance to mass transfer exists in both the liquid and gas phases.

EFFECT OF CONCENTRATION LEVEL UPON MASS TRANSFER

Two forms of Fick's first law may be written for a binary mixture of components A and B:

$$J_A^* = -cD_{AB}\nabla x_A \qquad (1)$$

$$J_A^0 = -(D_{AB}/\tilde{V}_A)\nabla\varphi_A \qquad (2)$$

The value of D_{AB} in the above two equations is the same, even if there are gradients in temperature and pressure, as long as $\tilde{V}_A$ remains constant and the substance to which Equation (2) is applied is incompressible and has a zero coefficient of expansion (*12, 15*).

It is convenient to use Equation (1) for mass transfer situations where the group cD_{AB} does not vary significantly throughout the fluid. This is found to be true for most gases at moderate pressures when temperature gradients are not large. The conditions for Equations (1) and (2) to be equivalent frequently exist in liquid solutions; therefore the application of Equation (2) is often advantageous since a composition-dependent density does not affect that equation directly.

Equations (1) and (2) may be converted to forms involving N_A and N_B:

$$N_A - x_A(N_A + N_B) = -cD_{AB}\nabla x_A \qquad (3)$$

$$N_A - \varphi_A(N_A + N_B\tilde{V}_B/\tilde{V}_A) = -(D_{AB}/\tilde{V}_A)\nabla\varphi_A \qquad (4)$$

If $(N_A + N_B)$ is not zero, then it is obvious from Equation (3) that N_A is dependent upon x_A as well as upon ∇x_A. If Equation (3) is written at the gas-liquid interface, then the interfacial flux of A is concentration dependent; this is what is meant by the concentration level effect. Since $x_A < 1$, an increase in concentration level of the transferred species will result in an increase in total flux if $(N_A + N_B)$ is of the same sign as N_A. Similar reasoning involving volumetric fluxes applies to Equation (4).

EFFECT OF FLUX LEVEL UPON MASS TRANSFER

Whereas the effect of concentration level can be demonstrated by considering the magnitude of certain terms in the Fick's law expression, the effect of high flux or, equivalently, high concentration gradient enters in a more subtle manner. For low flux situations, the equations of motion and the mass transfer equations may be solved independently and sequentially. For a high flux mass transfer situation, however, the mass flux must be considered as an additional velocity term, comparable in magnitude to the velocities present in the absence of mass transfer; hence, the equations of motion and mass transport can no longer be decoupled. This type of solution yields a different concentration profile shape from the low flux solution. On the other hand, the shape of the concentration profile is not altered by high solute concentration level alone; the concentration profile for a small concentration gradient at a high concentration level is similar to that for a small concentration gradient at a low concentration level.

In order to differentiate between the low and high flux solutions, it is convenient to employ for gaseous systems the local mass transfer coefficient defined by Bird et al. (*2*):

Michael W. Clark is with the Dow Chemical Company, Walnut Creek, California.

$$\dot{k}_x = \frac{N_{A0} - x_{A0}(N_{A0} + N_{B0})}{x_{A0} - x_{A\infty}} \qquad (5)$$

The definition of $\dot{k}_x$ compensates for the concentration level effect, since $\dot{k}_x$ is necessarily equal to $-(D_{AB}/\Delta x_A)(\partial x_A/\partial y)_{y=0}$. $\dot{k}_x$ is determined by the interfacial composition gradient.

Since most mass transfer correlations are based on experiments performed under low flux conditions, it is convenient to predict the high flux performance by applying a numerical correction factor to the low flux results. For this purpose, the dimensionless variables R_{AB}, Φ_{AB} and θ_{AB} defined by Bird et al. (2) are helpful. Both R_{AB} and Φ_{AB} ($= R_{AB}\,\theta_{AB}$) are dimensionless expressions for the net interfacial mass flux. θ_{AB} is the correction factor which, when applied to a low flux expression for the mass transfer coefficient, yields the mass transfer coefficient at a high mass flux. Thus, if one is able to obtain a solution to the high flux problem for a given flow situation, the results can be presented graphically in terms of any two of these three variables.

The correction factors for various models do not differ greatly at moderate flux levels. At present, high flux solutions exist for three important flow geometries: the film theory, for which the solution was first carried out by Lewis and Chang (*11*); the penetration theory, for which the solution was obtained by Arnold (*1*); and laminar boundary-layer theory. The resultant correction factors are given in Figures 21-7-2 and 21-7-3 in the text by Bird et al. (2).

Unfortunately, none of the existing high flux solutions were directly applicable to the velocity profiles encountered in this work. Byers and King (3) have shown that for short contact times, a flow geometry consisting of a finite interfacial velocity plus a linear velocity gradient away from the interface will closely approximate the exact, parabolic solution for the gaseous phase in concurrent, gas-liquid channel flow. In view of this, a high flux solution was carried out for the case of a linear velocity profile leading away from a stagnant interface in a semi-infinite fluid (the Leveque model). This case and the penetration model represent the two extremes of the finite interfacial velocity–linear velocity gradient flow geometry.

Because of the complexity of the high flux Leveque problem, the equations were solved in finite-difference form by using the Crank-Nicholson six-point implicit formula (*10*). The results, when placed in the dimensionless form of θ_{AB} vs. R_{AB}, are shown in Figure 1. The result for the laminar boundary-layer model at a Schmidt number of 1.5 and that for the penetration model are also shown. As can be seen, the curve for the Leveque model differs very little from the results for the penetration model, and therefore either of these could be used to predict the high flux behavior for the gaseous phase of the experimental equipment, provided the contact times are not too long.

Another complication that frequently arises at high flux levels is a variation of important physical properties across the concentration range between the interface and the bulk fluid. However, this is not a necessary consequence of increased flux level and therefore can be considered separately.

PREVIOUS WORK

A number of previous studies have been made of the effects of high flux and high concentration level on rates of mass transfer to and from turbulent flows. Colburn and

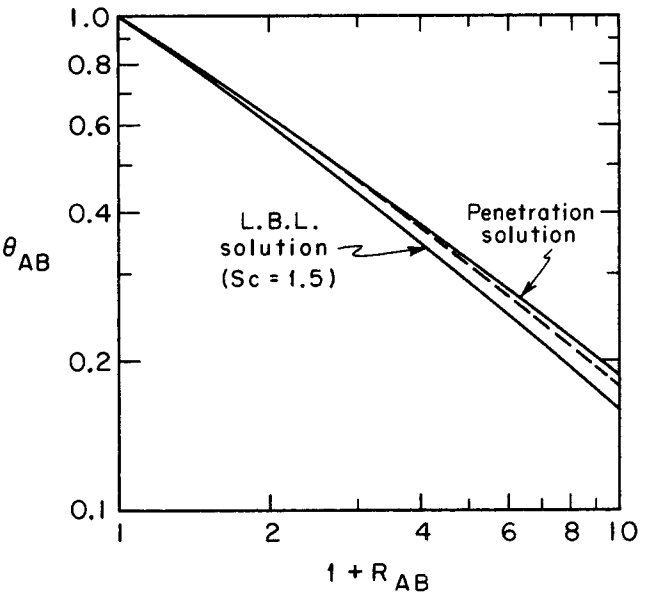

Fig. 1. Effect of high mass flux on the mass transfer coefficient for the Leveque model (dashed curve).

Drew (*8*) developed the P_{BM} correction factor which is predicted by the film model for the case where $N_{B0} = 0$ and evaluated this correction factor for the evaporation of water into a turbulent air stream. Similar experiments concerning evaporation into turbulent gas flows were carried out by Cairns and Roper (*5*), Westkaemper and White (*20*), Shulman and Delaney (*17*), and by Wasan and Wilke (*19*). These investigators arrived at different conclusions regarding the appropriate correction factor to be applied. Vivian and Behrman (*18*) surveyed the previous work and reported results of their own for the absorption and desorption of ammonia in a short wetted wall column. Their conclusion was that the P_{BM} correction factor is compatible with the available experimental data for mass transfer into a turbulent gas stream when $N_{B0} = 0$.

There have been fewer experimental studies of high flux and high concentration level mass transfer in laminar flows. Emanuel and Olander (*9*), Ranz and Dickson (*16*), and Mendelson and Yerazunis (*13*) all examined situations to which laminar boundary-layer theory should apply and achieved varying degrees of success in matching their results to theoretical predictions.

EXPERIMENTAL APPARATUS

The equipment used in this study was similar to that described by Byers and King (*4*). The gas-liquid contacting device (Figure 2) was a horizontal rectangular duct, with a large width-to-height ratio. The gas and liquid phases passed through this channel in stratified, concurrent, laminar flow with both the phases having equal depth of ½ in. An entry section served to establish velocity profiles in each phase. The inside dimensions of the test section were: length = 18.0 in., width = 3.0 in., and height = 1.0 in. (½ in. in each phase). As can be seen in Figure 2, provision was made for sampling the temperature and composition at several points along the exposure length, at ½, 10, and 17.5 in. from the inlet. The temperature and composition probes were mounted on micrometer barrels that were inserted into the holes indicated in Figure 2. As a result, these variables could be determined quite accurately as functions of vertical position.

A schematic diagram of the experimental apparatus is given in Figure 3. The evaporating liquid was continuously circulated through a closed loop system, in which provisions were made for adjusting the temperature and flow rate and for

adding liquid to the system. The gas was continuously withdrawn from cylinders through a pressure regulator, passed through a heater for temperature control, and was then contacted with the liquid phase. After the exposure, the two phases were separated by a thin metallic divider plate. Additional details concerning this apparatus are given elsewhere (*4, 7*).

Important features of the apparatus were:

1. The use of chromel-constantan thermocouple temperature probes. These probes were constructed from 5 mil diameter wires with 0.5 mil Teflon coating, threaded through 23 mil diameter stainless steel tubing. The probe was bent so that the tip end was horizontal into the gas flow. The final 0.6 in. of the probe wires were left bare, extending beyond the stainless steel support tube. The low conductivity metals chosen and the horizontal probe configuration were necessary to overcome the problems of registering accurate temperatures in a low velocity gas flow field.
2. A modification of the inlet calming section design to provide for better insulation of the inlet gas stream from the inlet liquid stream. Byers and King used a thin metallic divider plate separating the gas and liquid. In the present work, the gas entered along a parabolic flow path which kept the inlet gas and inlet liquid physically far apart until near the end of the inlet divider. As a result, the final entry angle of the gas was 6 deg.
3. Windings of nichrome wire placed around the gas entry section. A carefully controlled current passed through these wires could be used to make up for heat losses from the channel and maintain an adiabatic wall condition more closely.

In the present work nitrogen was employed as the gas-phase feed stream. Hydrocarbons were used for the liquid feed. *n*-pentane and isopentane served as volatile liquid species, while a linear paraffinic hydrocarbon mixture served as a nonvolatile liquid species. This mixture, henceforth referred to as *n*-tridecane, was in reality a stillcut from the isosieve process composed of 16 mole % n-$C_{12}H_{26}$, 58% n-$C_{13}H_{28}$, 25% n-C_{14}-H_{30} and 1% n-$C_{15}H_{32}$.

Gas chromatography was used for gas- and liquid-phase analyses. An aerograph A-90-P2 chromatograph was employed with a column composed of silicone oil SE-30 on firebrick support.

LOW FLUX HEAT AND MASS TRANSFER EXPERIMENTS

The previous work by Byers and King (*3, 4*) found good agreement between convective diffusion theory and experimental results for low flux, low concentration level mass transfer. Evaporation rates for the cases of gas-phase control and of resistances distributed between the gas and liquid phases were successfully analyzed.

In order to confirm the applicability of this approach for the case of heat transfer in the absence of mass transfer, a number of experimental runs were carried out in which heat was transferred from a warm nitrogen stream (approximately 32°C., inlet) to a nonvolatile liquid (*n*-tridecane) at approximately 20°C., inlet. Temperature measurements with the inlet probe indicated that heat transfer in the entering section amounted to the equivalent of an extra 1.5 in. of channel contact length. Under adiabatic wall conditions, the experimental average heat transfer coefficients, which were obtained through integration of the entrance and exit temperature profiles, agreed with the theoretically predicted coefficients quite well, with an average relative percent deviation of only 2.8% (*7*). Evaporation of *n*-pentane from *n*-tridecane into nitrogen at low solute concentration levels was also carried out, with close agreement between the experimental and theoretical mass transfer coefficients. Details of these heat and mass transfer measurements are given elsewhere (*7*).

EFFECT OF MASS TRANSFER UPON INTERFACIAL TEMPERATURE

The high flux mass transfer results were obtained by vaporizing two pure fluids, *n*-pentane and isopentane, into nitrogen. Both of these liquids have boiling points that are only slightly above the run conditions. Consequently, the mass flux levels were quite high, and the effect of the latent heat of evaporation upon the temperature profiles could not be ignored. A calculation similar to that outlined by Modine, et al. (*14*) was found to yield an acceptable prediction of the experimentally observed decrease in the liquid interfacial temperature, under conditions where cellular convection cells did not arise in the liquid phase (see part II). The first step in the procedure is to calculate the mass transfer rate by assuming a constant interfacial temperature equal to the inlet liquid temperature and by using the value of x_{A0} in the gas at the interface predicted by the vapor pressure relationship. The rate of heat consumption at the interface is directly related to the evaporation rate through the latent heat of vaporization. Since the liquid phase obeys the penetration model closely, the temperature difference between the interface and the bulk liquid can be related quantitatively to the rate of heat consumption at the interface by means of the solutions given by Carslaw and Jaeger (*6*) for transient heat conduction in a semi-infinite slab.

Having determined the value of T_0, one can go to the vapor pressure curve of the fluid in question, obtain a new value of x_{A0} corresponding to the new value of T_0, and repeat the above calculations. This iterative approach usually converged to a constant value of T_0 after three

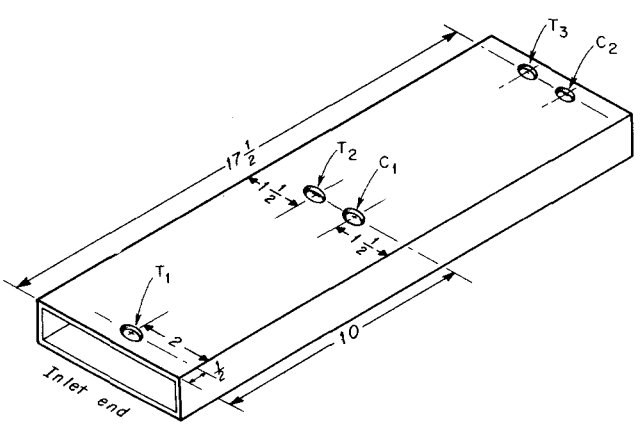

Fig. 2. Schematic of channel for gas-liquid contact, showing dimensions and probe locations.

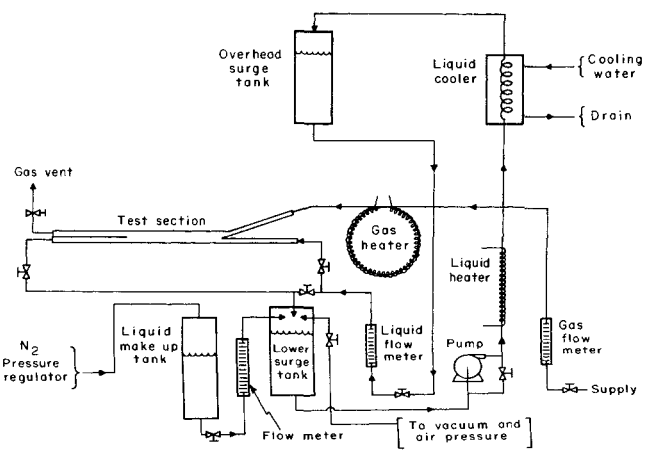

Fig. 3. Experimental apparatus.

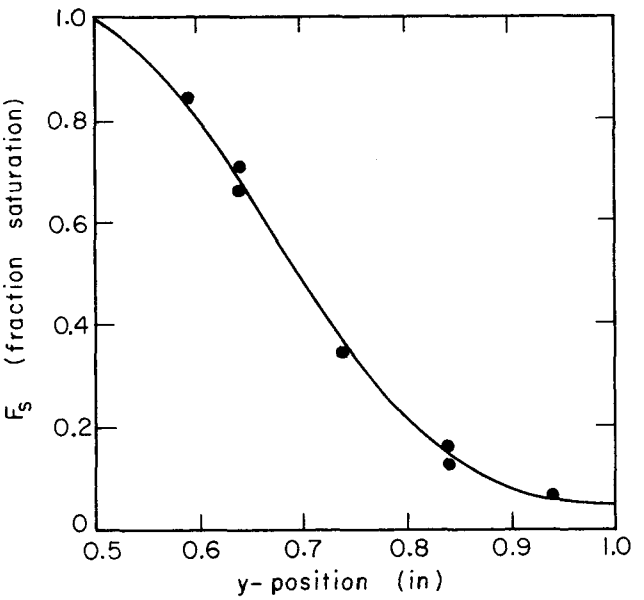

Fig. 4. Exit concentration profile for run No. 240. $x_{A0} = 0.584$. System: *n*-pentane/nitrogen.

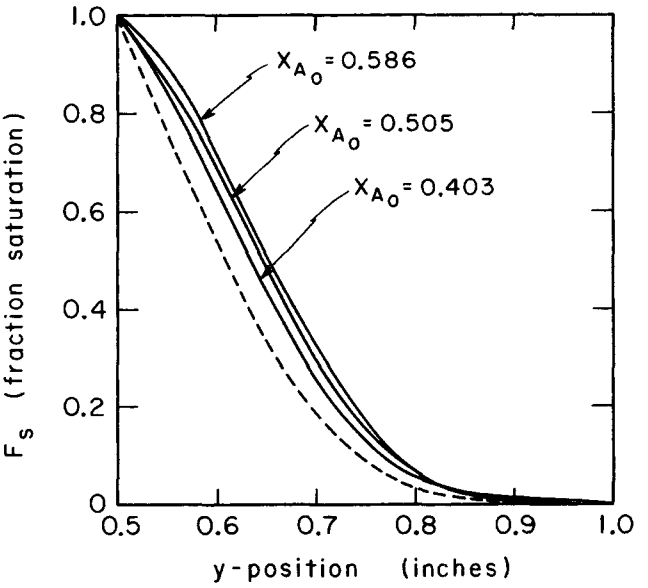

Fig. 5. Exit concentration profile for various interfacial mole fractions.

or four iterations. Details of this calculational method are given elsewhere (7).

For the interpretation of high-flux evaporation data, interfacial temperatures obtained with the temperature probes were employed to obtain the equilibrium partial pressure of the evaporating species. It was found that the interfacial temperature would change by no more than 0.1° to 0.4°C along the channel. An average temperature was used to obtain x_{A0} for converting the cup-mixing mole fraction to F_s.

HIGH FLUX MASS TRANSFER RESULTS

The high flux level mass transfer data were obtained in two ways, by the measurement of gas-phase concentration profiles and by the measurement of cup-mixing concentrations. The mole fraction of the volatile species was obtained by sampling a continuous flow from either the concentration probe or the exit stream, by using the gas chromatograph. From three to six chromatograms were obtained for each experimental point, and an average value was calculated. The chromatograms for a single point usually gave between 5 and 10% spread.

Figure 4 represents an experimental concentration profile taken at the exit probe for a gas-phase interfacial mole fraction of 0.584. The experimental system was *n*-pentane evaporating into pure nitrogen. The fraction saturation F_s is based upon the experimentally observed interfacial temperature according to the formula

$$F_s = x_A/x_{A0} \tag{6}$$

Figure 5 is a comparison of several experimental concentration profiles taken at the same flow conditions, with varying values of interfacial concentration. The increase in overall transfer rate and the decrease of k_x as the value of x_{A0} is raised can easily be seen. For comparison the low flux, low concentration profile for the same flow conditions is given by the dashed curve.

In order to compare the experimentally obtained profiles with a theoretical approach, it was first necessary to integrate these profiles to obtain a cup-mixing concentration according to the equation

$$x_{A,\text{ cup mix}} = \int_0^b \frac{u_x(y)x_A(y)dy}{b\,U_{x,\text{ avg}}} \tag{7}$$

The experimental cup-mixing mole fraction was then converted to a fraction saturation by dividing it by the equilibrium mole fraction at the interfacial conditions. A theoretical value of the fraction saturation was obtained in the following manner.

First, a low flux value of the average fraction saturation was obtained based upon the steady state flow conditions which would have occurred in the absence of mass transfer. For this purpose the numerical solution outlined by Byers and King (3) was used. The variation in gas viscosity due to composition and temperature was generally small and was ignored by presuming that the gas-phase velocity profile was parbaolic, as would occur for constant viscosity. The fraction saturation is directly related to the average mass transfer coefficient based on the inlet driving force for the low flux, low concentration level case by the equations

$$k_{x,\text{ avg}}\,x_{A0} = N_{A0,\text{ avg}} \tag{8}$$

and

$$N_{A0,\text{ avg}}\,L = c\,x_{A,\text{ cup mix}}\,U_{x,\text{ avg}}\,b \tag{9}$$

$$F_{s,\text{ avg}} = \frac{k_{x,\text{ avg}}\,L}{c\,U_{x,\text{ avg}}\,b} \tag{10}$$

Manipulating the above two equations along with Equations (5) and (7), we see that the correction factors which have been derived for the average mass transfer coefficient, to account for flux level and interfacial concentration level, are also applicable to the cup-mixing concentration.

Thus, the flux correction can be applied by multiplying the right-hand side of Equation (10) by θ_{AB}, and the concentration factor is applied by dividing by $(1 - x_{A0})$. The appropriate value of θ_{AB} was obtained by first calculating R_{AB} for the experimental conditions, and then by using Figure 1 to obtain θ_{AB}. Actually, owing to the existence of a finite interfacial velocity, the correct value of θ_{AB} should lie somewhere between the penetration and Leveque solutions. Since the difference between the two is quite small, the penetration model was utilized in all calculations.

For the prediction of mass transfer coefficients, gas-phase diffusivities were computed by the approaches of Wilke and Lee (21) and of Bird and Slattery (2). The diffusivity of the nitrogen-*n*-pentane system was taken as 0.0882 sq. cm./sec., while that for the nitrogen-isopen-

Table 1. High Flux Experimental Results

Graetz No. $(D_{AB}L/U_{x,avg}b^2)$	x_{A0}	Experimental F_s	Theoretical* F_s	% error
Evaporation of *n*-Pentane into N_2				
0.0454	0.403	0.248	0.235	+5.6
0.0454	0.418	0.278	0.239	+14.0
0.0454	0.505	0.291	0.248	+14.8
0.0842	0.410	0.377	0.353	+6.4
0.0842	0.586	0.380	0.382	−0.5
0.0842	0.586	0.427	0.382	+10.5
0.1510	0.439	0.535	0.481	+10.1
0.1510	0.586	0.591	0.525	+11.2
0.0810	0.418	0.357	0.338	+5.3
Evaporation of Isopentane into N_2				
0.0956	0.560	0.402	0.400	+0.2
0.0956	0.655	0.435	0.421	+3.2
0.1368	0.560	0.490	0.483	+1.4
0.1368	0.681	0.488	0.516	−5.7
0.1368	0.740	0.509	0.536	−5.3
			Average percent error =	+5.1

* Based upon velocity profile which would occur in the absence of mass transfer.

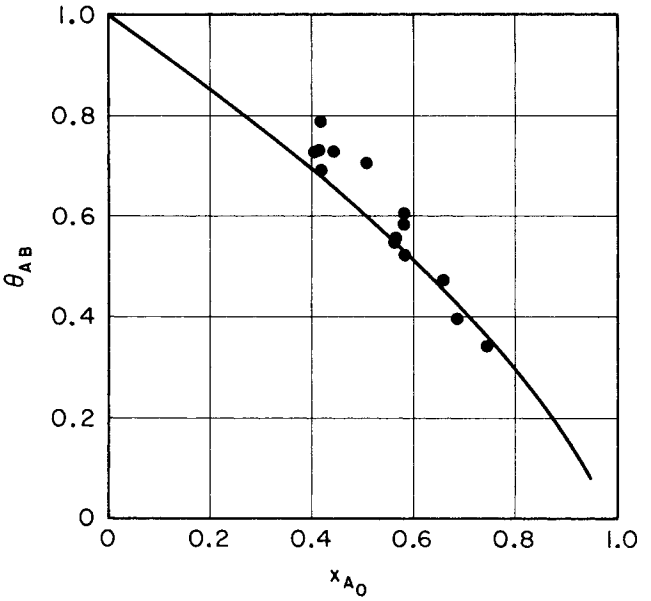

Fig. 6. Experimental values of high flux correction factors for the evaporation of *n*-pentane and isopentane into nitrogen.

tane system was taken as 0.0894 sq. cm./sec., both at 20°C. The vapor pressures of *n*-pentane and isopentane were taken as 418.8 and 570.6 mm. Hg, respectively, at 20°C. A tabulation of all experimental data and sources of physical properties is available elsewhere (7).

In addition to the integration of the experimental concentration profiles, a number of cup-mixing concentrations were obtained directly by sampling the exit gas stream. The overall experimental results are summarized in Table 1. The gas flow rate was varied to give results at different Graetz numbers; however, the liquid flow rate was held constant at 0.4 gal./min. The agreement between the calculational approach and the experimental results is quite good; however, there is some tendency for the experimental fraction saturation to be somewhat higher than the predicted values. This is not surprising, since a potentially important factor was ignored in the theoretical model. The experimental arrangement was one of confined flow; this meant that as the liquid phase evaporated, it contributed a significant amount of material and therefore acceleration to the gas phase in the region near the interface. It is difficult to predict the exact influence of this acceleration upon the transfer coefficients; however, the qualitative effect should be to increase the mass transfer into the gas phase. This increase in fraction saturation due to acceleration was calculated to be approximately 10% for $x_{A0} = 0.50$, if it is assumed that the velocity profile remains parabolic, that is, that the acceleration is uniform across the gas phase and that variations in viscosity can be ignored. As can be seen from the experimental results given in Table 1, a slight increase in the theoretical value of the fraction saturation would result in somewhat better agreement between the theoretical and experimental results.

If we assume that the concentration level correction is correctly given by dividing F_s by $(1 - x_{A0})$, then the experimental high flux results can be used to test the flux-level correction factor θ_{AB}. Figure 6 is a graph of θ_{AB} as a function of x_{A0}. The solid curve was obtained by using the penetration high flux solution, under the conditions of $N_{B0} = 0$, and $x_{A,} = 0$. The experimental data points tend to be a little high; however, this is probably due to the previously mentioned acceleration effect. The agreement is still fairly good, with the average relative error being ±6.2%.

NOTATION

b = channel half width, cm.
c = total concentration, g.moles/cc.
D_{AB} = diffusion coefficient in the binary system *A-B*, sq.cm./sec.
F_s = fraction saturation of the gas phase
J_A^0 = molar flux of species *A* relative to the volume average velocity, g.moles/sq.cm.sec.
J_A^* = molar flux of species *A* relative to the molar average velocity, g.moles/sq.cm.sec.
k_x = mass transfer coefficient at low flux conditions, based on mole fraction driving force, moles/sq.cm.-sec., $k_x = \lim (\overset{\bullet}{k_x})$ at $(N_{A0} + N_{B0}) = 0$
$\overset{\bullet}{k_x}$ = mass transfer coefficient, based on mole fraction driving force and applicable at high flux conditions, g.moles/sq.cm.-sec., defined by Equation (5)
L = exposure length, cm.
N_A = molar flux of component *A* relative to stationary coordinates, g.moles/sq.cm.-sec.
P_{BM} = log mean pressure of component *B*
R_{AB} = dimensionless flux ratio $= (N_{A0} + N_{B0})/\overset{\bullet}{k_x}$
T = temperature, °C.
$U_{x,\,avg}$ = average gas velocity in the x direction, cm./sec.
U_{int} = interfacial velocity in the x direction, cm./sec.
u_x = velocity in the x direction, cm./sec.
$\tilde{V}$ = partial molal volume
x = horizontal distance variable, cm.
x_A = mole fraction of component *A*, gas phase
y = vertical distance from the bottom of the channel, cm.

Greek Letters

Δ = difference between two quantities
θ_{AB} = dimensionless flux correction factor $= \overset{\bullet}{k_x}/k_x$
φ_A = volume fraction of component *A*
Φ_{AB} = dimensionless flux ratio $= (N_{A0} + N_{B0})/k_x$

∇ = vector differential operator

Subscripts

A, B = components A, B, etc.
AB = binary system composed of components A and B
avg = average value of a quantity
0 = evaluated at the interfacial position
∞ = quantity evaluated at a large distance from the gas-liquid interface, equivalent to inlet conditions

LITERATURE CITED

1. Arnold, J. H., *Trans. AIChE*, **40**, 361 (1944).
2. Bird, R. B., W. E. Stewart, and E. N. Lightfoot, "Transport Phenomena," John Wiley, New York (1960).
3. Byers, C. H., and C. J. King, *AIChE J.*, **13**, 628 (1967).
4. *Ibid.*, **13**, 637 (1967).
5. Cairns, R. C., and G. H. Roper, *Chem. Eng. Sci.*, **3**, 97 (1954).
6. Carslaw, H. S., and J. C. Jaeger, "Conduction of Heat in Solids," Oxford University Press, 2nd Ed., New York (1959).
7. Clark, M. W., and C. J. King, *U.S. Atomic Energy Comm.*, Rept. UCRL 17527 (1967).
8. Colburn, A. P., and T. B. Drew, *Trans. AIChE*, **33**, 197 (1937).
9. Emanuel, A. S., and D. R. Olander, *Intern. J. Heat Mass Transfer*, **7**, 539 (1964).
10. Lapidus, L., "Digital Computation for Chemical Engineers," McGraw-Hill, New York (1962).
11. Lewis, W. K., and C. K. Chang, *Trans. AIChE*, **21**, 127 (1928).
12. Lightfoot, E. N., and E. L. Cussler, Jr., *Chem. Eng. Progr. Symp. Ser.*, **61**, No. 58, 66 (1965).
13. Mendelson, H., and A. Yerazunis, *AIChE J.*, **11**, 834 (1965).
14. Modine, A. D., E. B. Parrish, and H. L. Toor, *ibid.*, **9**, 348 (1963).
15. Olander, D. R., *J. Phys. Chem.*, **67**, 1011 (1963).
16. Ranz, W. E., and P. F. Dickson, *Ind. Eng. Chem. Fundamentals*, **4**, 345 (1965).
17. Shulman, H. L., and L. J. Delaney, *AIChE J.*, **5**, 290 (1959).
18. Vivian, J. E., and W. C. Behrmann, *ibid.*, **11**, 656 (1965).
19. Wasan, D. T., and C. R. Wilke, *U.S. Atomic Energy Comm.*, Rept. UCRL-11629 (1964).
20. Westkaemper, L. E., and R. R. White, *AIChE J.*, **3**, 69 (1957).
21. Wilke, C. R., and C. Y. Lee, *Ind. Eng. Chem.*, **47**, 1253 (1955).

Part II. Liquid Mixtures

An approach has been developed for predicting rates of interphase mass transfer under conditions of high flux and high concentration level. A rectangular channel device has been used to measure rates of evaporation of four solutes, carbon disulfide, *n*-pentane, cyclopentane, and ethyl ether, from *n*-tridecane into flowing nitrogen. The evaporation rate of carbon disulfide agreed with the prediction of the interphase theory up to a carbon disulfide mole fraction of 0.30 in the bulk liquid. For the other three systems, a concentration gradient induced, surface tension driven cellular convection served to increase liquid-phase coefficients substantially. A correlation was obtained for the effect of this cellular motion on the liquid-phase mass transfer coefficient.

In part I of this series, the prediction of evaporation rates was simplified by the lack of liquid-phase mass transfer resistance. The calculation of mass transfer rates for the evaporation of liquid mixtures is considerably more complex, since the mass transfer resistance can lie in both the gas and liquid phases. The interfacial gas-phase composition is a function of interfacial temperature and the ratio of the mass transfer coefficients in the two phases. The problem requires the simultaneous solution of the convective transport equations for both phases. If the complicating factors of high flux and high concentration level are also important, the problem becomes still more difficult.

The experimental equipment utilized in this study was the same rectangular duct described in part I. A number of different volatile compounds were vaporized from a flowing nonvolatile solvent (*n*-tridecane) into a flowing nitrogen stream. The mass transfer conditions could be varied by changing either the nature or the concentration of the evaporating substance, or the temperature. Since the equipment has already demonstrated predictable behavior with respect to the stream flow variables (7 to 9), the flow conditions were fixed for all runs. The inlet nitrogen flow rate was held at 166 cc./sec., while the feed liquid flow was 0.400 gal./min. The interfacial temperature was controlled to within 0.2°C. of a constant value for each solute system.

INTERPHASE MASS TRANSFER

The first major contributions toward the solution of the general two-phase resistance, mass transfer problem were made by Lewis (*16*) and Whitman (27). Their approach resulted in a simple addition of independently measured individual phase resistances to yield the overall mass transfer resistance. There are a number of criteria which must be satisfied in order for the additivity of independently measured individual phase resistances to be valid (*12*). The effects of deviations from these criteria tend to cancel out one another in simple equipment providing only a single exposure of the contacting phases, particularly when the additivity principle is applied to the average rather than the local mass transfer coefficients. In complex contacting equipment, such as packed and plate columns, the departure from additivity can be much more severe.

For concurrent flow in the device used in this study, the additivity of resistances principle is accurate to better than 2% for low flux and low concentration levels, provided the the Graetz number ($D_{AB}L/U_{avg}b^2$) is less than 0.50 (*8, 9*). Independently measured resistances tend to be additive if the individual coefficients have similar functionalities with respect to exposure time, or length of contact between phases. Since the high flux and high concentration level corrections do not affect the x direction functionality of the individual phase mass transfer coefficients, the additivity principle should work as well under conditions of high flux and high concentration level, provided the correction factors for these effects are properly applied.

A convenient and accurate assumption for most liquid-phase mass transfer calculations is that of constant partial molal volume, which leads to a liquid-phase mass transfer coefficient based on volume fraction driving forces: